EUROPHYSICS LETTERS 1 August 1998

Europhys. Lett., **43** (3), pp. 235-240 (1998)

Lattice BGK simulation of sound waves

J. M. Buick, C. A. Greated and D. M. Campbell

Department of Physics and Astronomy, The University of Edinburgh
Mayfield Road, Edinburgh EH9 3JZ, UK

(received 29 January 1998; accepted in final form 16 June 1998)

PACS. 02.70−c – Computational techniques.
PACS. 43.20Hq – Velocity and attenuation of acoustic waves.
PACS. 43.25+y – Nonlinear acoustics, macrosonics.

Abstract. – We consider the application of the lattice Boltzmann BGK model to simulate sound waves in situations where the density variation is small compared to the mean density. Linear sound waves are simulated in two different situations: a plane wave propagating in an unbound region; and a wave in a tube. For both cases the behaviour of the simulated waves is found to be in good agreement with analytic expressions. Non-linear sound waves are also simulated and are seen to display the expected features.

In the past few years the lattice Boltzmann model (LBM) has been used to simulate a variety of isothermal, incompressible fluid flows [1,2]. It is well established that the LBM satisfies the incompressible Navier-Stokes and continuity equation although, like its predecessor the lattice gas model (LGM), it is generally considered to be applicable in the low Mach number limit to flows where there is a density variation which is small compared to the mean density [3,4]. In this letter we consider a new class of problems, the simulation of sound waves. Here there is a clear density variation, although in many circumstances this is small compared to the mean density and an incompressible approximation can yield good results, even when non-linear sound waves are modelled. The LGM has been shown to be effective under such circumstances [3,5-7] despite the inherent noise which is not present in LBM simulations.

The LBM employed here uses a two-dimensional hexagonal grid in which each node is connected to its six nearest neighbours by six unit vectors $\boldsymbol{e}_i$, $i = 1, 2, \ldots, 6$. The technique involves simulating the Boltzmann equation [8,9]

$$f_i(\boldsymbol{r} + \boldsymbol{e}_i, t+1) - f_i(\boldsymbol{r}, t) = \Omega_i(\boldsymbol{r}, t)\,, \quad i = 0,\, 1, \ldots\, 6. \tag{1}$$

The functions $f_i(\boldsymbol{r}, t)$, $i = 1, \ldots, 6$ are the distribution functions along the links $\boldsymbol{e}_i$ at site $\boldsymbol{r}$ and time t while $f_0(\boldsymbol{r}, t)$ is a rest particle distribution function. From these distribution functions the fluid density, ρ, and velocity, $\boldsymbol{u}$, can be found according to the relations

$$\rho = \sum_i f_i \quad \text{and} \quad \rho u_\alpha = \sum_i f_i e_{i\alpha}\,, \tag{2}$$

where the vector $\boldsymbol{e}_0$ is the null vector and we have used Roman subscripts as labels and Greek subscripts to represent components. Here we consider the simplest form for Ω_i, the "collision term", the single relaxation time or BGK operator [10,8,11]:

$$\Omega_i(\boldsymbol{r}, t) = -\frac{1}{\tau}\Big[f_i(\boldsymbol{r}, t) - \overline{f}_i(\boldsymbol{r}, t)\Big]\,, \tag{3}$$

where $\overline{f}_i$ is the equilibrium distribution function and τ is the relaxation time. The relaxation time, τ, is constrained to be greater than $1/2$ and the equilibrium distribution takes the form

$$\overline{f}_i(\boldsymbol{r},t) = \rho\left(\frac{1}{12}+\frac{1}{3}\boldsymbol{e}_i\cdot\boldsymbol{u}+\frac{2}{3}(\boldsymbol{e}_i\cdot\boldsymbol{u})^2-\frac{u^2}{6}\right), i=1,\ldots,b \quad \text{and} \quad \overline{f}_0(\boldsymbol{r},t)=\rho\left(\frac{1}{2}-u^2\right). \tag{4}$$

With this equilibrium distribution the incompressible Navier-Stokes equation can be recovered:

$$\partial_t\rho u_\alpha+\partial_\beta\rho u_\beta u_\alpha=-\partial_\alpha\frac{\rho}{4}+\nu\partial_\beta\partial_\beta\rho u_\alpha+\partial_\alpha\zeta\partial_\beta\rho u_\beta\,, \tag{5}$$

where $\nu=\zeta=(\tau-1/2)/4$ are the kinematic shear and bulk viscosities. The pressure term in eq. (5) is $p=\rho/4$ which, for a perfect gas, gives the speed of sound as $c_0=(1/4)^{1/2}$.

Other numerical techniques are available for simulating acoustic waves and these have been applied to a large variety of problems. These include compressible and thermal BGK models [12, 13] which are more complex than the approach taken here but which would be required if a large density or temperature change occurs. Two of the most common methods are the finite-difference method (FDM) and the boundary element method (BEM); these numerical schemes and their application to modelling sound are described in refs. [14] and [15] and references therein. FDM is a well-established procedure for solving time-independent problems where the accuracy of the simulation is related to truncation order of the Taylor expansion. This relation does not hold for time-dependent acoustics problems and so the accuracy of any simulation, regardless of the order, is brought into question. It is also necessary to use a technique which explicitly preserves the dispersion relation [16]. The BEM reduces a D-dimensional simulation to discretizing the $(D-1)$-dimensional boundary of the problem. A major drawback of the BEM is the "non-uniqueness" problem. Modifications which have been proposed to overcome this tend to be complicated and computationally inefficient or cannot be guaranteed to find the correct solution [17]. The BEM also becomes more complicated if the boundary is complex. The LBM can be applied to acoustical problems in the same way as it has been applied to simulated fluid flow. This makes it ideally suited to simulate the interaction between a sound field and an external flow, even in a situation where one is several orders of magnitude larger than the other. The simplicity of the LBM means that the complexity of the geometry, both at the boundary and of internal obstacles, does not change the efficiency of the algorithm.

A plain sound wave with wave number k will propagate with frequency ω, where $\omega=kc_0$ and c_0 is the speed of sound in the propagation medium. The wave will be damped due to internal viscous dissipation at a rate per period of [18, 19]

$$\alpha=\frac{2(2\pi)^3E_{\mathrm{w}}}{3}\,, \tag{6}$$

where E_{w} is a dimensionless variable,

$$E_{\mathrm{w}}=\frac{\eta}{c_0k\lambda^2} \tag{7}$$

and $\eta=\nu+\zeta/2$. In a two-dimensional tube of width y_1 the speed of sound is altered to [18]

$$c=c_0\left(1-\frac{1}{y_1}\sqrt{\frac{\nu}{2\omega}}\right). \tag{8}$$

Thus a sound wave with wavelength λ in a two-dimensional pipe of width y_1 will have a dimensionless frequency $\omega'=\omega/(c_0k)$ which is a solution of $(\omega')^{3/2}-(\omega')^{1/2}=-E_{\mathrm{p}}^{1/2}/\sqrt{2}$,

where

$$E_{\mathrm{p}} = \frac{\nu}{c_0 k y_1^2} \tag{9}$$

is a dimensionless variable. The solution we require (that is $\omega' \to 1$ as $E_{\mathrm{p}} \to 0$) is

$$\omega' = \frac{4}{3}\cos^2\left[\frac{1}{3}\cos^{-1}\left(-\frac{3\sqrt{3}}{2\sqrt{2}}E_{\mathrm{p}}^{1/2}\right)\right]. \tag{10}$$

For such a wave the damping rate per period caused by the confinement of the pipe is $\alpha = \pi(2E_{\mathrm{p}}\omega')^{1/2}$, combining this with the internal dissipation, eq. (6), gives the total damping rate per period:

$$\alpha = \pi\sqrt{2E_{\mathrm{p}}\omega'} + (2\pi)^3 E_{\mathrm{p}} F^2, \tag{11}$$

where F is the ratio of the pipe width to the wavelength of the sound, $F = y_1/\lambda$. These results are true provided the pipe is not so narrow that the layer immediately affected by the friction extends over the whole tube, that is provided $E_{\mathrm{p}} \ll 1$ [18].

Sound waves were simulated using the LBM described above; both plane waves propagating in the x-direction in an unbound fluid and waves in a horizontal two-dimensional pipe were considered. In each case the wavelength of the wave was the same as the number of grid points in the x-direction and periodic boundary conditions were applied at $x = 0$ and $x = \lambda$. The periodic boundary condition wraps round the grid at $x = 0$ and $x = \lambda$, that is $f_i|_{x=\lambda+1}$ is mapped to $f_i|_{x=0}$ and $f_i|_{x=-1}$ is mapped to $f_i|_{x=\lambda}$. The other two grid edges, at $y = 0$ and $y = n$, where set as periodic boundaries and no-slip boundaries [20] when the unbound fluid and the pipe were considered, respectively. When the pipe is simulated $n = y_1$, otherwise 40 grid points were used in the y-direction; this corresponds to $n = 40 \times \sqrt{3}/2$ since each row of sites is separated by $\sqrt{3}/2$ lattice units (the separation of the sites) on a hexagonal lattice. The sound wave was then initialised with density $\rho = \rho_0 + \delta\rho\sin(kx)$, $u_x = \delta\rho c_0/\rho_0 \sin(kx)$ and $u_y = 0$. The density and velocity were then measured at this point $x = \lambda/4$ at subsequent times. The relative density variation $\rho' = \delta\rho/\rho_0$ is shown as a function of the relative time $t' = t\omega/2\pi$ in fig. 1 for a wave propagating in an unbound fluid and in fig. 2 for a sound wave in a pipe. An initial relative density of 0.001 was used for the unbound wave while a larger value of $\rho' = 0.01$ was used for the bound wave where a higher rate of damping is expected. The relative velocity $u' = u_x/c_0$ was seen to behave identically to ρ' in all the simulations.

The results in fig. 1 are for ten periods of oscillation after an initial 100 periods. In this time the wave has been damped to about 3/4 of its initial value and the sinusoidal variation of the density (and the velocity) are seen to be maintained over this length of time. The results in fig. 2 show the significantly higher damping rate which occurs within a pipe. In order to assess the frequency and damping rate the density results were fitted to a damped co-sine. The quality of the fit, and hence of the frequency ω and damping rate per period α obtained from the fitting process, can be assessed by calculating the root-mean-square deviation between the simulation results and the fitted curve. This was found to be 0.009% and 0.007% of the mean density for the results shown in figs. 1 and 2. This was repeated for a selection of waves with different wavelengths, viscosities and pipe thicknesses, in each case at least the first ten periods of oscillation were used in the fitting process. The relative frequencies and the damping rate per period are shown in figs. 3 and 4 for the unbound and bound waves, respectively. The results in fig. 3 show that for the range of wavelengths and viscosities used here the measured frequency is within 0.05% of $c_0 k$, as expected. The damping rate per period is seen to vary linearly with E_{w} and is in good agreement with eq. (6). In fig. 4 the relative frequency is seen to vary from ~ 1 at low values of E_{p} (corresponding to a wide pipe in a

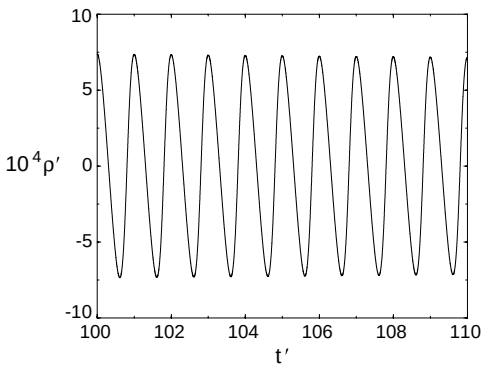

Fig. 1

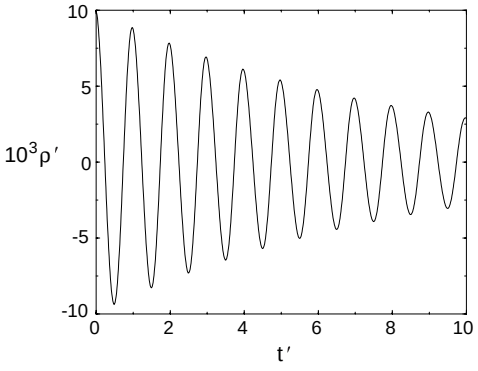

Fig. 2

Fig. 1. – Relative density and velocity of a plane sound wave with wavelength 2000 lattice units and initial relative density 0.001 propagating in an unbound fluid. Ten periods are shown after the wave has propagated for 100 periods. The simulation was run with $\tau = 0.75$ giving $\nu = 0.0625$.

Fig. 2. – Relative density and velocity of a plane sound wave with wavelength 100 lattice units and relative density 0.01 propagating in a two-dimensional pipe of width $37\sqrt{3}/2$ lattice units. The first ten periods of oscillation are shown. The simulation was run with $\tau = 0.75$ giving $\nu = 0.0625$.

low-viscosity fluid) to ~ 0.91 at the largest value of E_p (corresponding to a narrow pipe in a high-viscosity fluid), a change of almost 10%. Also in fig. 4 the damping rate per period is shown as a function of E_p for different values of F; again there is good agreement between the simulation results and the analytic expressions. The values of the viscosity were selected to best display the attenuation of the wave while ensuring the oscillations are maintained for a significant number of periods, in many cases it is desirable to reduce the viscosity as much as possible. In practice this is limited by the values of λ and ρ', the lowest value considered, although not presented here, is $\nu = 0.01$. The linear sound waves presented in figs. 1 to 4 have an initial relative pressure of either 0.01 or 0.001. To consider the applicability of such simulations to real situations we consider the relative pressure variation in sound waves. The sound pressure level is given by $\mathrm{SPL} = 20\log(P/P_\mathrm{ref})$, where P is the measured pressure of

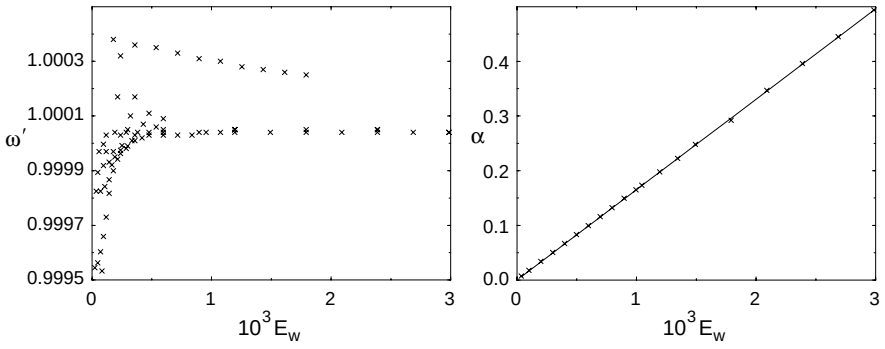

Fig. 3. – The relative frequency, ω', and damping rate per period, α, for an unbound wave as a function of the dimensionless parameter E_w. The solid line is the analytic expression in eq. (6). The results are for $0.025 \leq \nu \leq 0.125$ and $20 \leq \lambda \leq 100$.

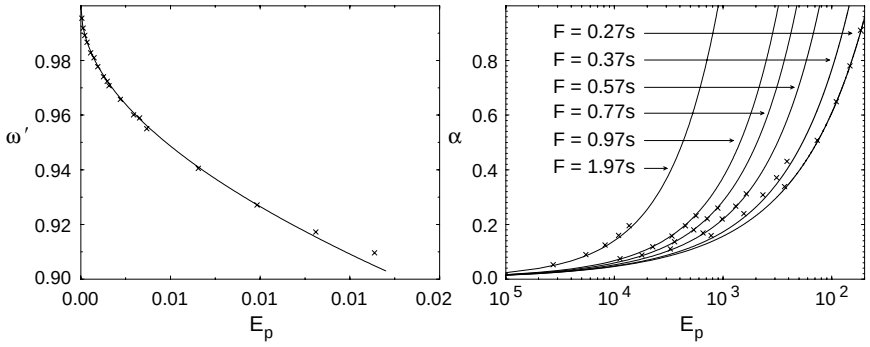

Fig. 4. – The relative frequency, ω', and damping rate per period, α, for a bound wave for different values of F, the ratio of the pipe width to the wavelength, as a function of the dimensionless parameter $E_{\rm p}$. The solid lines are the analytical expressions in eqs. (10) and (11). The results are for $0.025 \leq \nu \leq 0.125$, $27s \leq y_1 \leq 197s$ and $\lambda = 100$, $s = \sqrt{3}/2$.

the sound wave and $P_{\rm ref}$ is a reference pressure which in air is usually taken to be 2×10^{-5} Pa; this is approximately the pressure of a 1000 Hz pure tone which is barely audible to a person with unimpaired hearing. Now, 120 dB is the loudest sound which can legally be heard in the workplace without requiring ear defenders to be worn. This corresponds to a pressure variation of 20 Pa, relative to atmospheric pressure of 1×10^5 Pa. Thus the relative pressure variation of a 120 dB sound wave is 0.0002 which is smaller than the value used here.

We now consider sound waves with a larger density variation. At 160 dB the relative density variation is 2% of the mean density. At this sound level we expect our incompressible approximation to still be valid and we expect the resulting sound waves to exhibit non-linear effects [21]. This is demonstrated in fig. 5 for an unbound sound wave with an initial relative density of 0.02 and wavelength 500 lattice units. The wave was initialised with a sinusoidal density and velocity variation, however after five or six periods the non-linear effects become noticeable and after twenty periods the characteristic "N"-shape variation in the density and velocity is observed. In fig. 5 the relative time is $t' = tc_0/\lambda$. Thus fig. 5 also shows a small

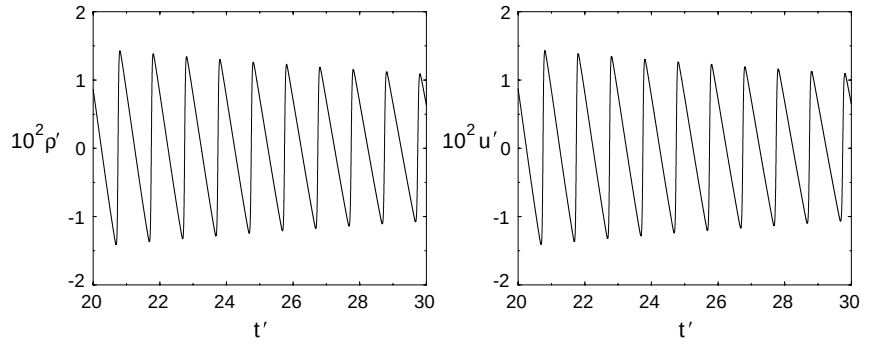

Fig. 5. – Relative density and velocity of a plane sound wave with wavelength 500 lattice units and initial relative density 0.02 propagating in an unbound fluid. Approximately ten periods are shown after the wave has propagated for approximately twenty periods, the viscosity is $\nu = 0.0625$. The similarity of ρ' and u', which was found in all the simulations, can be observed.

change in the wave period. The non-linear deviations from a sine-wave observed in fig. 5 are typical of results obtained elsewhere for a 160 dB standing wave in a tube [21] and in the slide section of a trombone [22] at pressures of the same order as the pressure used here.

In conclusion, we have considered the simulation of sound waves using a BGK lattice Boltzmann model. It is seen that once a linear sound wave has been initialised it continues to oscillate in the expected manner for at least 110 periods. We have also considered the rate at which the wave is attenuated in an unbound fluid and in a two-dimensional pipe. In both cases the simulations were in good agreement with the theoretical expressions. The speed of sound was also considered. In an unbound fluid the relative frequency, ω/c_0k, was seen to be 1 showing agreement between the lattice Boltzmann speed of sound and the ratio ω/k of the sound wave. In a two-dimensional pipe the change in the speed of sound, seen here through the relative frequency changing from unity (when the wave number is fixed), was also observed and was in agreement with the theoretical expression. Non-linear sound waves at a higher intensity have also been simulated. These sound waves show the same qualitative features as have been observed elsewhere. We have shown that the LBM can be usefully employed for the numerical study of sound wave propagation.

***

The work presented here was partially funded by EPSRC. The authors would also like to thank the Edinburgh Parallel Computing Centre (EPCC) for providing time on the Cray T3D.

REFERENCES

[1] Benzi R., Succi S. and Vergassola M., *Phys. Rep.*, **222** (1992) 145.
[2] J. L. Lebowitz, S. A. Orszag and Y. H. Qian (Editors), *J. Stat. Phys.*, Vol. **81**, *Special issue on Lattice-based models and related topics* (1995).
[3] Stansell P. and Greated C. A., *Phys. Fluids*, **9** (1997) 3288.
[4] Martys N. S. and Chen H., *Phys. Rev. E*, **53** (1996) 743.
[5] Chen H., Chen S. and Doolen G. D., *Phys. Lett. A*, **140** (1989) 161.
[6] Lavallee P., *Phys. Lett. A*, **163** (1992) 392.
[7] Sudo Y. and Sparrow V. W., *AIAA J.*, **33** (1995) 1582.
[8] Chen S., Chen H., Martinez D. and Matthaeus W., *Phys. Rev. Lett.*, **67** (1991) 3776.
[9] Qian Y. H., d' Humières D. and Lallemand P., *Europhys. Lett.*, **17** (1992) 479.
[10] Bhatnagar P. L., Gross E. P. and Krook M., *Phys. Rev.*, **94** (1954) 511.
[11] Chen S., Wang Z., Shan X. and Doolen G. D., *J. Stat. Phys.*, **68** (1986) 379.
[12] McNamara G. R., Garcia A. L. and Alder B. J., *J. Stat. Phys.*, **87** (1997) 1111.
[13] Xu K., Kim C., Martinelli L. and Jameson A., AIAA-96-0525 (1996).
[14] Tam C. K. W., *AIAA J.*, **33** (1995) 1788.
[15] Habault D. M. L., in *Proceedings of the 15th International Congress on Acoustics*, edited by M. Newman (Trondheim, Norway) 1995, p. 61.
[16] Tam C. K. W. and Webb J. C., *J. Comp. Phys.*, **107** (1993) 262.
[17] Wu T. W. and Seybert A. F., *J. Acoust. Soc. Am.*, **90** (1991) 1608.
[18] Lord Rayleigh, in *The Theory of Sound* (Macmillan and Co., London) 1929.
[19] Kinsler L. E., Frey A. R., Coppens A. B. and Sanders J. V., in *Fundamentals of Acoustics* (John Wiley & Sons) 1980.
[20] Noble D. R., Chen S., Georgiadis J. G. and Buckius R. O., *Phys. Fluids*, **7** (1995) 203.
[21] Maa D.-Y. and Liu K., *J. Acoust. Soc. Am.*, **98** (1995) 2753.
[22] Gilbert J. and Petiot J.-F., in *Proc. ISMA'97*, edited by A. Myers (Edinburgh) 1997, p. 391.